COMPUTING CONFORMAL INVARIANTS: PERIOD MATRICES*

XIANFENG GU†, YALIN WANG‡, AND SHING-TUNG YAU§

Abstract. This work introduces a system of algorithms to compute period matrices for general surfaces with arbitrary topologies. The algorithms are intrinsic to the geometry, and independent of surface representations. The computation is efficient, stable and practical for real applications. The algorithms are experimented on real surfaces including human faces and sculptures, and applied to surface identification problems. It is the first work that is both theoretically solid, and practically robust and accurate to handle real surfaces with arbitrary topologies.

Keywords: Conformal Structure, Period Matrix, Conformal Geometry, Mesh.

1. Introduction. Geometric matching and surface classification are fundamental problems in computer vision, computer graphics, and medical imaging fields. Conformal geometry provides solid theoretic foundation to solve these problems. All orientable surfaces are Riemann surfaces, hence, by Riemann Uniformization theorem, they can be conformally mapped to three canonical spaces: the sphere, the plane and the Poincaré space. Surface matching problems can be converted to planar image matching problems on these canonical spaces.

Surfaces can be classified by the conformal transformation group. If two surfaces can be conformally mapped to each other, they are conformally equivalent. The classification by conformal equivalence is much refiner than topological classification, and more flexible than classification by rigid motions. The complete conformal invariants are described by a g by g complex matrix, the so called *period matrix*, where g is the genus of the surface.

We tested our algorithms on real surfaces laser scanned from real sculptures and ones reconstructed from medical images. The computation process is intrinsic to the geometry, and independent of the data structure, insensitive to noise. The process does not require the computation of curvatures, so it is much more efficient than traditional methods.

To the best of knowledge, the algorithm in this work is the first practical algorithm that is able to handle real surfaces with arbitrary topologies. The computation is efficient and stable, and the period matrices obtained are accurate.

1.1. Previous Work. Conformal geometry has been applied in computer graphics for texture mapping purposes. The algorithms for computing conformal maps from a topological disks to the plane have been studied in [4, 12, 13, 1]. In the medical

---

(a) Original Surface   (b) Conformal map to   (c) Texture mapped
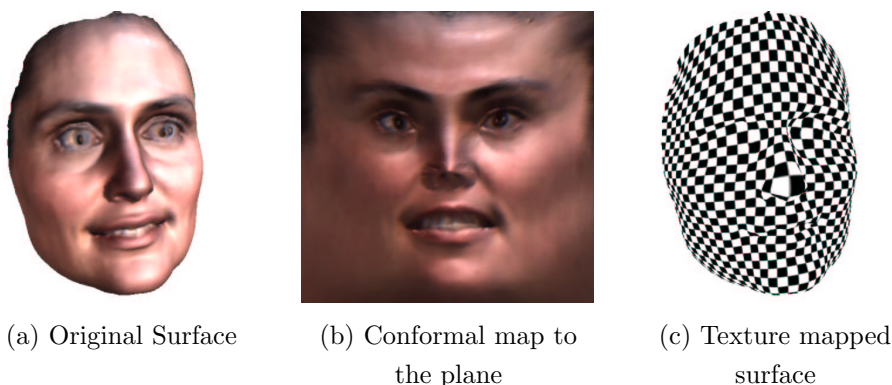   the plane   surface

Fig. 2.1. *Conformal mapping. The original surface is a real human face (a), which is conformally mapped to a square (b). A checker board texture is mapped back to the face. All the right angles on the texture are preserved on (c).*

imaging field, [2, 10] introduce a method for computing conformal map between a closed genus zero surface to the sphere.

For surfaces with arbitrary topologies, Gu and Yau introduce an algorithm based on Hodge theory. The algorithm for computing conformal structures of real surfaces has been introduced in [7]. Then the method is applied to brain mapping [5, 6, 14] in medical imaging, surface classification in [9], and global surface parameterizations in [8].

1.2. Organization of the Paper. In section 2, the concept of conformal mapping will be explained briefly. In section 3, the main concepts and definitions in conformal geometry will be systematically introduced in the setting of discrete surfaces. Section 4 introduces the algorithms in details. Section 5 generalizes the algorithms to surfaces with boundaries. Section 6 demonstrates the experimental results on real surfaces. We summarize the paper in the final section 7.

2. Riemann Surface. This section concentrates on the concepts of *conformal map*, *conformal structure* and *Riemann surface*, which are introduced in [3] and [11].

Suppose S_1 and S_2 are two regular surfaces, parameterized by (x^1, x^2). Let a mapping $\phi : S_1 \rightarrow S_2$ be represented in the local coordinates as $\phi(x^1, x^2) = (\phi^1(x^1, x^2), \phi^2(x^1, x^2))$.

Suppose the first fundamental forms (Riemannian metrics) of S_1 and S_2 are

$$ds_1^2 = \sum_{ij} g_{ij} dx^i dx^j \tag{1}$$

$$ds_2^2 = \sum_{ij} \tilde{g}_{ij} dx^i dx^j. \tag{2}$$

The pull back metric on S_1 induced by ϕ is

$$(3) \qquad \phi^* ds_2^2 = \sum_{mn} \sum_{ij} \tilde{g}_{ij}(\phi(x^1, x^2)) \frac{\partial \phi^i}{\partial x^m} \frac{\partial \phi^j}{\partial x^n} dx^m dx^n.$$

DEFINITION 2.1 (conformal mapping). *ϕ is a conformal mapping between S_1 and S_2, if there exists a positive function $\lambda(x^1, x^2)$ such that*

$$(4) \qquad ds_1^2 = \lambda(x^1, x^2) \phi^* ds_2^2.$$

Especially, if the map from S_1 to the local coordinate (x_1, x_2) plane is conformal, we say (x_1, x_2) is a conformal coordinate of S_1, or *isothermal coordinate*. Using conformal coordinates, the metric can be formulated as $ds^2 = \lambda(x_1, x_2)(dx_1^2 + dx_2^2)$.

Figure 2.1 demonstrates a conformal map between a human face surface and a square on the plane. The conformality is illustrated by texture mapping a checkerboard to the surface. It is easy to verify that all right angles on the checkerboard are preserved on the surface.

DEFINITION 2.2 (conformal structure). *A conformal structure of a surface S is an atlas, where each chart is a conformal coordinates of S, and the transition function between two charts are holomorphic.*

DEFINITION 2.3 (Riemann surface). *A surface which admits a conformal structure, is called a Riemann surface.*

All orientable surfaces are Riemann surfaces. If there is a conformal mapping $\phi : S_1 \to S_2$ between two surfaces S_1 and S_2, then S_1 and S_2 are conformally equivalent, namely, they share the same conformal structure. The complete invariants of conformal structures can be represented as period matrices, which will be explained in details in the next section.

The main goal of this paper is to design algorithms to compute period matrices. In practice, the surfaces are represented by triangular meshes. In the next section, we will define the concepts of conformal geometry in the discrete surface cases.

3. Discrete Riemann Surface. Suppose K is a simplicial complex, and a mapping $f : |K| \to R^3$ embeds $|K|$ in R^3, then $M = (K, f)$ is called a *triangular mesh*. K_n are the sets of *n-simplicies*, where $n = 0, 1, 2$. We use σ^n to denote a n-simplex, $\sigma^n = [v_0, v_1, \cdots, v_n]$, where $v_i \in K_0$.

3.1. Homology Group. We define *chain spaces* as the linear combination of simplices,

$$(5) \qquad C_n(M) = \{\sum_j c_j \sigma_j^n | c_j \in \mathbb{Z}, \sigma_j^n \in K_n\}, n = 0, 1, 2.$$

The elements in C_n are called *n-chain*s. Notably, the summation of all faces $\sum_k f_k$ is in C_2. We also use M to denote this special 2-chain. Next we define boundary operators among the chain spaces.

DEFINITION 3.1 (boundary operator). *Boundary operator* $\partial_n : C_n \to C_{n-1}$ *is a linear operator. Suppose* $\sigma^n \in K_n$, $\sigma^n = [v_0, v_1, \cdots, v_{n-1}]$, *then*

$$(6) \qquad \partial_n \sigma^n = \sum_{i=0}^{n-1} (-1)^i [v_0, \cdots, v_{i-1}, v_{i+1}, \cdots, v_{n-1}].$$

Then for a n-chain in C_n, *the boundary operator is defined as*

$$(7) \qquad \partial_n \sum c_i \sigma_i^n = \sum c_i \partial_n \sigma_i^n.$$

We use $ker\partial_1 \subset C_1$ to denote the null space of ∂_1, which represents all the closed curves on M. We use $img\partial_2 \subset C_1$ to denote the image space of ∂_2, representing all possible surface patch boundaries. It is easy to verify that all boundaries of surface patches are closed curves, namely

$$(8) \qquad \partial_1 \cdot \partial_2 = 0.$$

Hence $img\partial_2 \subset ker\partial_1$.

DEFINITION 3.2 (homology group). *The homology group of* M $H_n(M, \mathbb{Z})$ *is defined as*

$$(9) \qquad H_n(M, \mathbb{Z}) = \frac{ker\partial_n}{img\partial_{n+1}}.$$

Intuitively, $H_1(M, \mathbb{Z})$ represents all the closed loops which are not the boundaries of any surface patch on M. The topology of M is determined by $H_0(M, \mathbb{Z}), H_1(M, \mathbb{Z})$, and $H_2(M, \mathbb{Z})$.

Let M be a closed mesh of genus g, and $B = \{\gamma_1, \gamma_2, \ldots, \gamma_{2g}\}$ be an arbitrary basis of its homology group. We define the entries of the *intersection matrix* C of B as

$$(10) \qquad c_{ij} = -\gamma_i \cdot \gamma_j$$

where the dot denotes the algebraic number of intersections, counting $+1$ when the direction of the cross product of the tangent vectors of r_i and r_j at the intersection point is consistent with the normal direction and -1 otherwise.

3.2. Cohomology Group. Then we consider the homeomorphisms between chain spaces to R, which we can call *co-chain spaces*,

$$(11) \qquad C^n(M) = Hom(C_n, \mathbb{R}), n = 0, 1, 2,$$

where $Hom(C_n, R)$ means the set of all homeomorphisms between C_n to R. The elements in C^n are called *n-cochains* or *n-forms*. Similar to the boundary operators among chain spaces, we can define the *coboundary* operators $\delta_n : C^n \to C^{n+1}$ as

the dual operators to ∂_n. Suppose $\omega_n \in C^n$ is an *n-form* and $c_{n+1} \in C_{n+1}$ is an *n+1-chain*, then

$$(\delta_n \omega_n)(c_{n+1}) = \omega_n(\partial_{n+1} c_{n+1}). \tag{12}$$

It is easy to verify that $\delta_1 \cdot \delta_0 = 0$.

DEFINITION 3.3 (cohomology group). *The cohomology group $H^n(M, \mathbb{R})$ is defined as*

$$H^n(M, \mathbb{R}) = \frac{\ker\delta_n}{\mathrm{img}\delta_{n-1}}. \tag{13}$$

1-forms in $ker\delta^1$ are called *closed 1-forms* and 1-forms in $img\delta^0$ are called *exact 1-forms*. Two close 1-forms are called *cohomologous* if they differ by an exact 1-form. Cohomology group $H^1(M, \mathbb{R})$ is isomorphic to homology group $H_1(M, \mathbb{Z})$.

We can naturally define *integration* of an n-form along an n-chain. Suppose $c_n \in C_n$ and $\omega_n \in C^n$, then the integration is denoted as

$$< \omega_n, c_n >= \omega_n(c_n). \tag{14}$$

The boundary and coboundary operators are related by the *Stokes' formula*

$$< \omega_{k-1}, \partial_k c_k >=< \delta^{k-1} \omega_{k-1}, c_k > . \tag{15}$$

3.3. Wedge Product. Cohomology group is not only a group, but also a ring. Besides addition, there are also product operators for 1-forms.

DEFINITION 3.4 (wedge product). *Wedge product is a bilinear operator $\wedge : C^1 \times C^1 \to C^2$. Suppose $f \in K_2$ is a face on M, $\partial_2 f = e_0 + e_1 + e_2$, $\omega, \tau \in C^1$, then*

$$\omega \wedge \tau(f) = \frac{1}{6} \begin{vmatrix} \omega(e_0) & \omega(e_1) & \omega(e_2) \\ \tau(e_0) & \tau(e_1) & \tau(e_2) \\ 1 & 1 & 1 \end{vmatrix}. \tag{16}$$

We can define star wedge product operator in a similar way,

DEFINITION 3.5 (star wedge product). *A bilinear operator star wedge product $\wedge^* : C^1 \times C^1 \to C^2$ is defined as follows: suppose $f \in K_2$, the lengths of three edges are l_0, l_1, l_2 and the area of f is A, then*

$$\omega \wedge^* \gamma(f) = \Omega G \Gamma^t, \tag{17}$$

where

$$\Omega = (\omega(e_0), \omega(e_1), \omega(e_2)) \tag{18}$$

$$\Gamma = (\gamma(e_0), \gamma(e_1), \gamma(e_2)) \tag{19}$$

and quadratic form G has the form

$$G = \frac{1}{24s} \begin{pmatrix} -4l_0^2 & l_0^2 + l_1^2 - l_2^2 & l_0^2 + l_2^2 - l_1^2 \\ l_1^2 + l_0^2 - l_2^2 & -4l_1^2 & l_1^2 + l_2^2 - l_0^2 \\ l_2^2 + l_0^2 - l_1^2 & l_2^2 + l_1^2 - l_0^2 & -4l_2^2 \end{pmatrix}. \tag{20}$$

3.4. Harmonic 1-forms. We can associate the so called *harmonic energy* with all closed 1-forms.

DEFINITION 3.6 (harmonic energy). *Suppose $\omega \in C^1$, and we define the harmonic energy of ω as*

$$(21) \qquad E(\omega) = \sum_{e \in K_1} w_e \omega(e)^2,$$

where w_e is defined in the following way: suppose there are two faces f_0, f_1 attached to an edge e, then angles α, β are on f_0, f_1 against e respectively, then

$$(22) \qquad w_e = \frac{1}{2}(cot\alpha + cot\beta).$$

Suppose e is a boundary edge, $e \in \partial_2 M$, then e only attaches to one face f_0, in this case

$$(23) \qquad w_e = \frac{1}{2}cot\alpha.$$

In the following discussion, we always assume the triangulation of the mesh can guarantee the positiveness of w_e. The existence of such a triangulation can be proven by Riemann uniformization theorem.

DEFINITION 3.7 (harmonic 1-form). *A closed 1-form $\omega \in ker\delta^1$ is called a harmonic 1-form if it minimizes the harmonic energy.*

The *Laplacian* operator is an operator from C^1 to C^0, $\Delta : C^1 \to C^0$,

$$(24) \qquad \Delta\omega(u) = \sum_{[u,v] \in K_1} w_{[u,v]} \omega([u,v]).$$

A closed 1-form is harmonic if and only if its Laplacian is zero.

For each cohomology class, there only exists a unique harmonic 1-form. All harmonic 1-forms form a group, denoted as $\mathbb{H}$, which is isomorphic to $H^1(M, \mathbb{R})$.

DEFINITION 3.8 (dual harmonic 1-form basis). *Suppose M has a homology basis $\{r_1, r_2, \cdots, r_{2g}\}$ and a harmonic 1-form basis $\{\omega_1, \omega_2, \cdots, \omega_{2g}\}$, such that*

$$(25) \qquad < r_i, \omega_j > = -\gamma_i \cdot \gamma_j, i, j = 1, 2, \cdots, 2g,$$

where $-\gamma_i \cdot \gamma_j$ is the algebraic intersection number of γ_i and γ_j, then the homology basis and harmonic 1-form basis are said to be dual to each other.

3.5. Holomorphic 1-form. Given a harmonic 1-form $\omega \in \mathbb{H}(M)$, there is a unique *conjugate harmonic 1-form* ω^*, such that

$$(26) \qquad < \tau \wedge \omega^*, M > = < \tau \wedge^* \omega, M >, \forall \tau \in \mathbb{H}(M),$$

where M represents the special 2-chain consisting of all faces.

DEFINITION 3.9 (holomorphic 1-form). *Suppose ω is harmonic, and ω^* is its conjugate harmonic 1-form, then the pair $\omega + \sqrt{-1}\omega^*$ is called a holomorphic 1-form.*

All holomorphic 1-forms form a group $\Omega^1(M)$, which is isomorphic to $H^1(M, \mathbb{R})$. The basis of $\Omega^1(M)$ can be constructed directly from a basis of the harmonic 1-form group. Using previous notation, if $\{\omega_1, \omega_2, \cdots, \omega_{2g}\}$ is a basis of the harmonic 1-form group, then $\{\omega_1 + \sqrt{-1}\omega_1^*, \omega_2 + \sqrt{-1}\omega_2^*, \cdots, \omega_{2g} + \sqrt{-1}\omega_{2g}^*\}$ is a basis of $\Omega^1(M)$.

3.6. Period Matrix. The conformal structure of a surface can be represented by a special matrix, the *period matrix*.

DEFINITION 3.10 (period matrix). *Let S be a Riemann surface with genus g. Suppose $B = \{a_1, a_2, \cdots, a_g, b_1, b_2, \cdots, b_g\}$ is a canonical basis of $H_1(M, \mathbb{Z})$ and $B^* = \{\omega_1, \omega_2, \cdots, \omega_{2g}\}$ is the dual basis of $\Omega^1(M)$, then matrix $R = (r_{i,j})$ is called the period matrix, where*

(27) $$r_{ij} = \int_{b_i} \omega_j, i, j = 1, 2, \cdots, g.$$

4. Algorithms for Computing Period Matrices. This section introduces a series of practical algorithms to compute the period matrices. We first introduce the algorithms to compute the homology and cohomology of a surface, then the algorithms to compute harmonic one-forms and holomorphic one-forms.

4.1. Fundamental Domain. First we compute a fundamental domain D_M of a mesh M such that D_M is a topological disk and covers M once.

```
Algorithm 1. Computing a fundamental domain of mesh M.
Input : A mesh M.
Output: A fundamental domain D_M of M.
1. Choose an arbitrary face f₀ ∈ M, let D_M = f₀,
   ∂ D_M = ∂ f₀, put all the neighboring
   faces of f₀ which share an edge with f₀ to a queue Q.
2. While Q is not empty
   a.remove the first face f in Q, suppose
     ∂ f = e₀ + e₁ + e₂.
   b.D_M = D_M ∪ f.
   c.find the first eᵢ ∈ ∂ f, such that −eᵢ ∈ ∂ D_M,
     replace −eᵢ in ∂ D_M by {e_{i+1}, e_{i+2}}
     (keeping the order).
   d.put all the neighboring faces which share
     an edge with f and not in D_M or Q to Q.
3. Remove all adjacent oriented edges in ∂ D_M, which
   are opposite to each other, i.e. remove all pairs
   {e_k, −e_k} from ∂ D_M.
```

The resulting D_M includes all faces of M, which are sorted according to their queuing order. The non-oriented edges and vertices of the final boundary of D_M form a graph G, which is called a *cut graph*. We will compute the homology basis of G, namely $H_1(G, \mathbb{Z})$, which is equivalent to $H_1(M, \mathbb{Z})$.

4.2. Homology Basis. For the cut graph G, we can compute its homology generators, which is also the homology basis of M.

```
Algorithm 2. Computing a homology basis of M.
Input : A mesh M.
Output: Homology basis {γ₁, γ₂, ⋯, γ₂g}.
1. Compute a fundamental domain D_M of M, get the cut
   graph G.
2. Compute a spanning tree T of G, suppose
   G/T = {e₁, e₂, ⋯, e₂g}.
3. Choose a root vertex r ∈ T, depth first traverse T.
4. Suppose ∂ eᵢ = tᵢ − sᵢ, there are paths from root r
   to tᵢ and sᵢ, denoted as [r, tᵢ], and [r, sᵢ], then
   connect them to a loop γᵢ = [r, tᵢ] + [tᵢ, sᵢ] − [r, sᵢ].
5. Output { γ₁, γ₂, ⋯, γ₂g } as a basis of H₁(G, ℤ), also H₁(M, ℤ).
```

4.3. Computing Cohomology. We want to explicitly construct a basis for the cohomology group of M, $H^1(M, \mathbb{R})$. We will find a set of closed 1-forms $\{\omega_1, \omega_2, \cdots, \omega_{2g}\}$, such that

(28) $$< \gamma_i, \omega_j > = \delta_i^j.$$

where δ_i^j is the Kronecker symbol and $\{\gamma_i\}$ is a homology basis.

```
Algorithm 3. Computing a cohomology basis of M.
Input  : A Mesh M.
Output : Cohomology Basis {ω₁, ω₂, ⋯, ω₂g} .
1. Compute a fundamental domain D_M, the cut graph G,
   and a spanning tree T,G/T = {e₁, e₂, ⋯, e₂g }.
2. let ωᵢ( eᵢ ) = 1 and ω(e) = 0, for any edge e ∈ T.
3. Suppose D_M is ordered in the way that
   D_M = {f₁, f₂, ..., fₙ}, reverse the order of D_M to
   {fₙ, fₙ₋₁, ⋯, f₁}.
4. While D_M is not empty
   a. get the first face f of D_M, remove f from D_M,
        ∂ f = e₀ + e₁ + e₂.
   b. divide {eₖ} to two sets,
      Γ = {e ∈ ∂ f| − e ∈ ∂ D_M}, Π = {e ∈ ∂ f| − e ∉ ∂ D_M}.
   c. choose the value of ωᵢ(eₖ), eₖ ∈ Π  arbitrarily,
```

```
      such that ∑ₑ ∈ Π  ωᵢ( e )  =  − ∑ ₑ ∈ Γ   ωᵢ( e ),
      if Π is empty, then the right hand side is zero.
   d. Update the boundary of D_M, let
      ∂ D_M  =  ∂ D_M + ∂ f.
5. Output ωᵢ's.
```

Once we compute $\{\omega_1, \omega_2, \cdots, \omega_{2g}\}$, we can use linear transformation to transform them to the dual of homology basis $\{\gamma_1, \gamma_2, \cdots, \gamma_{2g}\}$, such that

$$(29) \qquad <\gamma_i, \omega_j> = -\gamma_i \cdot \gamma_j.$$

4.3.1. Computing Harmonic 1-forms. In this step, we would like to diffuse the 1-forms computed in the last step to be harmonic. Given a closed 1-form ω, we would like to find a function $f \in C^0(M)$, such that $\Delta(\omega + \delta f) = 0$.

```
Algorithm 4. Diffuse a closed 1-form to a harmonic 1-form.
Input  : A Mesh M, a closed 1-form ω.
Output : A harmonic 1-form, cohomologous to ω.
1. Choose f ∈ C⁰(M), build the linear system
   Δ (ω + δ f)  ≡  0.
2. Solve the above sparse linear system to get f.
3. Output ω + δ f.
```

where

$$(30) \qquad \Delta(\omega + \delta f)(u) = \sum_{[u,v]\in M} w_{u,v}(\omega([u,v]) + f(v) - f(u)), u \in K_0.$$

4.4. Computing Holomorphic 1-form Basis. For each harmonic 1-form, there exists a conjugate harmonic 1-form as defined in (26). The problem is to determine the uniqueness of the conjugate harmonic 1-form and find a way to compute it out.

Suppose $\{\omega_1, \omega_2, \cdots, \omega_{2g}\}$ is a harmonic 1-form basis. By definition, the conjugate harmonic 1-form ω^* should satisfy the following condition

$$(31) \qquad <\omega_i \wedge \omega^*, M> = <\omega_i \wedge^* \omega, M>, \forall \omega_i \in \mathbb{H}.$$

Because ω^* is also harmonic, we can represent it as a linear combination of ω_i's

$$(32) \qquad \omega^* = \sum_{k=1}^{2g} \lambda_k \omega_k,$$

and we get the following linear system

$$(33) \qquad \sum_{j=1}^{2g} \lambda_j <\omega_i \wedge \omega_j, M> = <\omega_i \wedge^* \omega, M>.$$

We want to show the linear system (33) is of full rank. We can prove the following theorem:

THEOREM 4.1. *For any harmonic 1-form, its conjugate harmonic 1-form exists and is unique.*

The proof is not elementary, we will use the duality between homology and co-homology from algebraic topology. Suppose the homology basis is $\{\gamma_1, \gamma_2, \cdots, \gamma_{2g}\}$, and

$$(34) \qquad\qquad <\omega_i, \gamma_j> = -\gamma_i \cdot \gamma_j,$$

then

$$(35) \qquad\qquad <\omega_i \wedge \omega_j, M> = \gamma_i \cdot \gamma_j,$$

where $\cdot$ represents the algebraic intersection number between two closed loops. Hence, the linear system in equation (33) is the intersection matrix of homology basis, which is definitely non-degenerated. The solution to (33) exists and is unique.

5. Surfaces With Boundaries. In this section, we want to generalize the method for closed meshes to meshes with boundaries. Given a surface M with boundary ∂M, $\partial M \neq \phi$, we want to compute the global conformal structure for M. We need to compute the holomorphic 1-form on M first.

5.1. Doubling. Given a surface M with boundaries ∂M, we can construct a symmetric closed surface $\bar{M}$, such that $\bar{M}$ covers M twice. That is, there exists an isometric projection $\pi : \bar{M} \rightarrow M$, which maps a face $\bar{f} \in \bar{M}$ isometrically to a face $f \in M$. For each face $f \in M$, there are two preimages in $\bar{M}$. We call $\bar{M}$ a *doubling* of M.

The following is the algorithm to compute the doubling of mesh with boundaries.

```
Algorithm 5. Compute Doubling of an Open Mesh
Input  : A mesh M with boundary
Output : The doubling of M, M̄
1. Make a copy of M, denoted as −M.
2. Reverse the orientation of −M.
3. For any boundary vertex u ∈ ∂ M, there exists a
   unique corresponding boundary vertex −u ∈ ∂−M,
   hence for any edge on e ∈ ∂M, there exists a
   unique boundary edge −e ∈ ∂(−M). Find all the
   correspondences.
4. Glue M and −M, make their corresponding boundary
   vertices and edges identical. The resulting mesh is
   the doubling M̄.
```

The doubling algorithm is very general for arbitrary surfaces with boundaries, and can be generalized to higher dimensional complexes. The purpose for doubling is to convert the surfaces with boundaries to closed symmetric surfaces.

Given a mesh M with boundaries, we would like to compute the basis of holomorphic 1-forms on M. We first compute the doubling $\bar{M}$ for M. For each interior vertex $u \in M$, there are two copies of u in $\bar{M}$, we denote them as u_1 and u_2, and say they are *dual* to each other, denoted as

(36) $$\bar{u}_1 = u_2, \bar{u}_2 = u_1.$$

For each boundary vertex $u \in \partial M$, there is only one copy in $\bar{M}$, we say u is dual to itself, i.e. $\bar{u} = u$.

We now compute the harmonic 1-forms on $\bar{M}$. According to Riemann surface theories [3], all symmetric harmonic 1-forms of $\bar{M}$

(37) $$\omega([u, v]) = \omega([\bar{u}, \bar{v}]).$$

are also harmonic 1-forms on M.

Define the dual operator for each harmonic 1-form ω as follows:

(38) $$\bar{\omega}([u, v]) = \omega([\bar{u}, \bar{v}]).$$

Any ω can be decomposed to a symmetric part and an asymmetric part

(39) $$\omega = \frac{1}{2}(\omega + \bar{\omega}) + \frac{1}{2}(\omega - \bar{\omega}),$$

where $\frac{1}{2}(\omega + \bar{\omega})$ is the symmetric part.

The following algorithm computes the holomorphic 1-form basis for surfaces with boundaries.

Algorithm 6. Computing a set of holomorphic 1-form
          basis for meshes with boundaries.
Input : Mesh M with boundaries
Output: Holomorphic 1-form basis for mesh M
        $\{\tau_1 + \sqrt{-1}\tau_1^*, \tau_2 + \sqrt{-1}\tau_2^*, \ \cdots, \ \tau_k + \sqrt{-1}\tau_k^* \ \}.$
1. Compute the doubling of M, $\bar{M}$.
2. Compute the harmonic 1-form basis of $\bar{M}$
    $\{\omega_1, \ \omega_2, \ \cdots, \ \omega_{2g} \ \}.$
3. Assign $\tau_i = \frac{1}{2}(\omega + \bar{\omega})$, remove redundant ones.
4. Compute conjugate harmonic 1-forms of τ_i,
    denoted as τ^*.
5. Output holomorphic basis
    $\{\tau_1 + \sqrt{-1}\tau_1^*, \tau_2 + \sqrt{-1}\tau_2^*, \ \cdots, \ \tau_k + \sqrt{-1}\tau_k^* \ \}.$

Then, we can use the holomorphic 1-form to compute the period matrix of M as described in previous section.

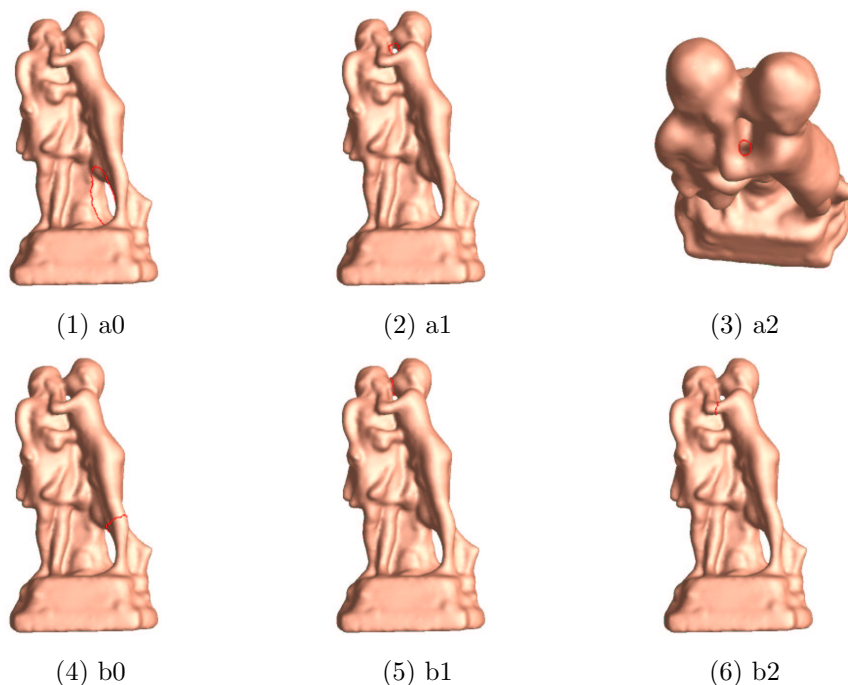| (1) a0 | (2) a1 | (3) a2 |

| (4) b0 | (5) b1 | (6) b2 |

FIG. 6.1. *The homology basis for the genus three sculpture model.*

6. Experimental Results. We tested our algorithms using real surfaces laser scanned from sculptures and human faces. The surfaces are represented using triangle meshes. The optimization is based on the conjugate gradient method, and the data structure is mainly half edge boundary representation.

6.1. Genus Three Sculpture Model. The sculpture model is shown in figure 6.1 with genus three. The canonical homology basis are also illustrated.

The period matrix is computed and display as the following:

$$(40) \qquad R = \begin{pmatrix} 0.0143 + 0.6991i & -0.0018 + 0.0068i & -0.0000 + 0.0067i \\ -0.0018 + 0.0064i & -0.0103 + 1.6003i & -0.0047 - 0.1894i \\ -0.0000 + 0.0067i & -0.0047 - 0.1898i & 0.0010 + 1.2844i \end{pmatrix}.$$

It is easy to verify that the matrix is symmetric, and the imaginary part is positive definite.

6.2. Human Face Surfaces With Feature Regions Removed. The face models are obtained by laser scanning real human faces. We locate the feature curves of the surfaces, and slice the surfaces along these feature curves. We double the resulting surfaces, and compute the period matrices of them.

Figure 6.2 (1) and (2) demonstrate the surfaces with feature regions removed. Figure 6.3 shows the holomorphic one-form basis for the female face surface using
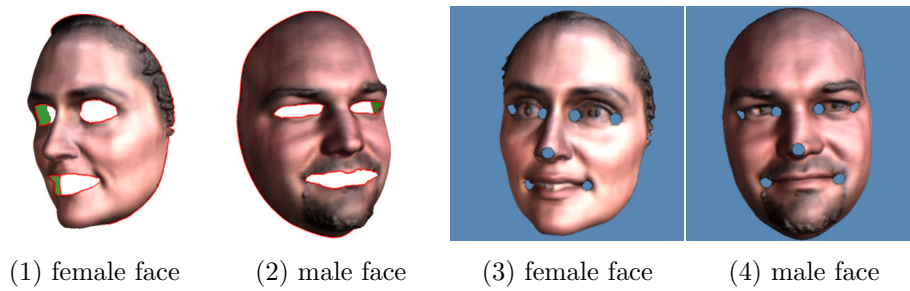
(1) female face   (2) male face   (3) female face   (4) male face

FIG. 6.2. *The human face surfaces are preprocessed. In (1) and (2), feature curves are located and the surfaces are sliced along these curves. In (3) and (4), feature points are computed first, then these feature points are removed. The surfaces can be identified by comparing the period matrices.*

texturemapping a checkerboard. Figure 6.4 shows the holomorphic one-form basis for the male face surface.
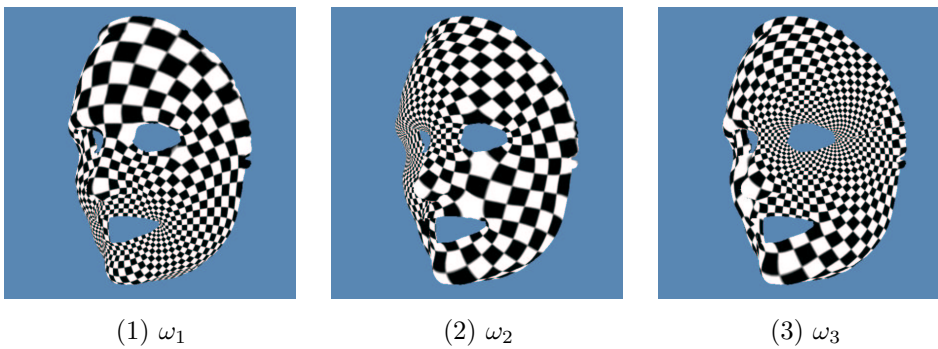

(1) ω_1 (2) ω_2 (3) ω_3

FIG. 6.3. *Holomorphic one-forms on female face model.*

(1) ω_1 (2) ω_1 (3) ω_3
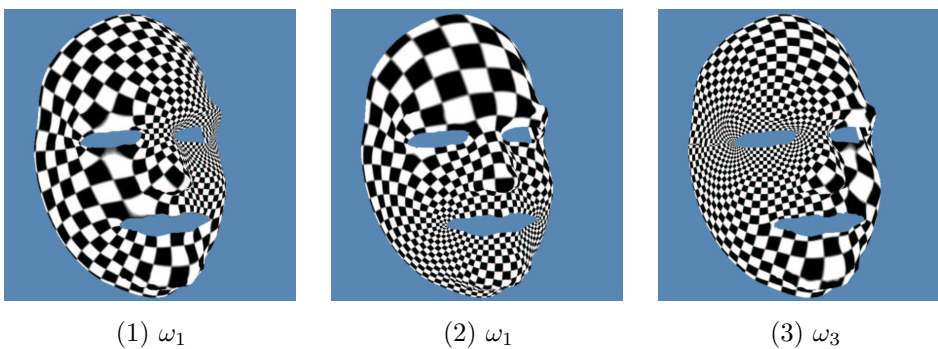
FIG. 6.4. *Holomorphic one-forms on male face model.*

The doubling surfaces are symmetric, the real parts of the period matrices are zero. In the following, only the imaginary parts are illustrated.

The male surface figure 6.2 (2) has the following period matrix:

$$
(41) \qquad \sqrt{-1} \begin{pmatrix} 0.6814 & 0.1642 & 0.1756 \\ 0.1642 & 0.4741 & 0.1582 \\ 0.1756 & 0.1582 & 0.6474 \end{pmatrix},
$$

the eigen vectors are

$$
(42) \qquad \begin{pmatrix} -0.6634 & -0.6915 & 0.2860 \\ -0.4321 & 0.0419 & -0.9009 \\ -0.6109 & 0.7212 & 0.3265 \end{pmatrix},
$$

the eigen values are

$$
(43) \qquad \begin{pmatrix} 0.9500 & 0 & 0 \\ 0 & 0.4833 & 0 \\ 0 & 0 & 0.3647 \end{pmatrix}.
$$

The period matrix for the female surface figure 6.2 (1) is

$$
(44) \qquad \sqrt{-1} \begin{pmatrix} 0.5335 & 0.1747 & 0.1775 \\ 0.1747 & 0.6464 & 0.1925 \\ 0.1775 & 0.1925 & 0.6540 \end{pmatrix},
$$

the eigenvectors are

$$
(45) \qquad \begin{pmatrix} 0.4861 & 0.8739 & -0.0052 \\ 0.6121 & -0.3448 & -0.7117 \\ 0.6237 & -0.3428 & 0.7025 \end{pmatrix},
$$

the eigenvalues are

$$
(46) \qquad \begin{pmatrix} 0.9812 & 0 & 0 \\ 0 & 0.3950 & 0 \\ 0 & 0 & 0.4577 \end{pmatrix}.
$$

6.3. Human Face Surfaces With Feature Points Removed. We locate the feature points on the male face and the female face manually, and punch small holes centered at the feature points as shown in figure 6.2(3) and (4). Then we compute the doubling the surfaces. Because the surfaces are symmetric, the real parts of the period matrices are zero. In the following we display the imaginary part.

The period matrix of the male surface in figure 6.2 (3) is

$$(47) \quad \begin{pmatrix} 0.9406 & 0.0821 & 0.3773 & 0.1518 & 0.1719 & 0.0859 & 0.2036 \\ 0.0821 & 0.9386 & 0.1551 & 0.3824 & 0.0860 & 0.1738 & 0.2096 \\ 0.3773 & 0.1551 & 1.1511 & 0.2953 & 0.2183 & 0.1488 & 0.3798 \\ 0.1518 & 0.3824 & 0.2953 & 1.1706 & 0.1477 & 0.2207 & 0.3873 \\ 0.1719 & 0.0860 & 0.2183 & 0.1477 & 0.9518 & 0.1654 & 0.2781 \\ 0.0859 & 0.1738 & 0.1488 & 0.2207 & 0.1654 & 0.9557 & 0.2855 \\ 0.2036 & 0.2096 & 0.3798 & 0.3873 & 0.2781 & 0.2855 & 1.3235 \end{pmatrix}.$$

The eigenvectors for the period matrix are

$$(48) \quad \begin{pmatrix} -0.2830 & -0.4842 & 0.3167 & -0.5459 & 0.4957 & 0.1635 & 0.1214 \\ -0.2889 & 0.4640 & 0.3150 & 0.4781 & 0.5758 & 0.1829 & -0.0919 \\ -0.4401 & -0.4742 & 0.3437 & 0.5116 & -0.3892 & -0.0946 & 0.2028 \\ -0.4495 & 0.4754 & 0.3566 & -0.4501 & -0.4372 & -0.0826 & -0.2103 \\ -0.2800 & -0.2319 & -0.3483 & 0.0698 & -0.0961 & 0.5278 & -0.6737 \\ -0.2848 & 0.2136 & -0.3648 & -0.0624 & -0.1269 & 0.5316 & 0.6615 \\ -0.5303 & 0.0040 & -0.5483 & -0.0155 & 0.2342 & -0.6024 & -0.0045 \end{pmatrix}.$$

The eigenvalues for the period matrix are

$$(49) \quad \begin{pmatrix} 2.4899 & 0 & 0 & 0 & 0 & 0 & 0 \\ 0 & 1.1251 & 0 & 0 & 0 & 0 & 0 \\ 0 & 0 & 0.9622 & 0 & 0 & 0 & 0 \\ 0 & 0 & 0 & 0.6338 & 0 & 0 & 0 \\ 0 & 0 & 0 & 0 & 0.6467 & 0 & 0 \\ 0 & 0 & 0 & 0 & 0 & 0.8217 & 0 \\ 0 & 0 & 0 & 0 & 0 & 0 & 0.7524 \end{pmatrix}.$$

The period matrix for the female face surface shown in figure 6.2 (4) is

$$(50) \quad \begin{pmatrix} 1.3530 & 0.2170 & 0.2821 & 0.3944 & 0.2956 & 0.3804 & 0.2053 \\ 0.2170 & 0.9282 & 0.0921 & 0.3711 & 0.1754 & 0.1617 & 0.0867 \\ 0.2821 & 0.0921 & 0.9641 & 0.1515 & 0.2020 & 0.1964 & 0.1464 \\ 0.3944 & 0.3711 & 0.1515 & 1.1036 & 0.2145 & 0.3190 & 0.1637 \\ 0.2956 & 0.1754 & 0.2020 & 0.2145 & 1.0087 & 0.1539 & 0.0897 \\ 0.3804 & 0.1617 & 0.1964 & 0.3190 & 0.1539 & 1.1237 & 0.3767 \\ 0.2053 & 0.0867 & 0.1464 & 0.1637 & 0.0897 & 0.3767 & 0.9245 \end{pmatrix}.$$

The eigen vectors are

$$
(51) \quad
\begin{pmatrix}
0.5418 & 0.1011 & -0.3935 & -0.7038 & 0.0688 & -0.2015 & -0.0272 \\
0.2868 & 0.4014 & 0.4411 & 0.1789 & -0.1561 & -0.4985 & -0.5071 \\
0.2803 & -0.0654 & -0.4871 & 0.3904 & -0.7230 & 0.0647 & -0.0203 \\
0.4359 & 0.3087 & 0.4704 & -0.0350 & -0.1747 & 0.3964 & 0.5518 \\
0.3022 & 0.3468 & -0.3613 & 0.5196 & 0.6158 & 0.0817 & 0.0446 \\
0.4327 & -0.5458 & 0.2067 & 0.0427 & 0.1553 & 0.4557 & -0.4883 \\
0.2775 & -0.5576 & 0.1366 & 0.2175 & 0.1192 & -0.5790 & 0.4436
\end{pmatrix}.
$$

The eigenvalues are

$$
(52) \quad
\begin{pmatrix}
2.5050 & 0 & 0 & 0 & 0 & 0 & 0 \\
0 & 1.0645 & 0 & 0 & 0 & 0 & 0 \\
0 & 0 & 0.9877 & 0 & 0 & 0 & 0 \\
0 & 0 & 0 & 0.8562 & 0 & 0 & 0 \\
0 & 0 & 0 & 0 & 0.7553 & 0 & 0 \\
0 & 0 & 0 & 0 & 0 & 0.6330 & 0 \\
0 & 0 & 0 & 0 & 0 & 0 & 0.6041
\end{pmatrix}.
$$

It is straightforward to identify two surfaces by comparing the eigenvalues of their period matrices. The computation process is global, and insensitive to the local noise, it is stable enough for real applications.

7. Summary and Conclusion. This paper introduces algorithms to compute period matrices for real surfaces. The algorithms compute the homology, cohomology, harmonic one-form basis and holomorphic one-form basis. The algorithms are intrinsic to the geometry of the surfaces, independent of the surface representation, and robust to the noise.

Period matrices can be used in surface classification and surface recognition. It is a challenging problem to qualitatively measure the dependency between the period matrices and the Riemann metric tensor. We will conduct future research along this direction and explore more applications of period matrices.

REFERENCES

[1] P. ALLIEZ, M. MEYER, AND M. DESBRUN, *Interactive geomety remeshing*, In: SIGGRAPH 02, pages 347–354, 2002.

[2] S. ANGENENT, S. HAKER, A. TANNENAUM, AND R. KIKINIS, *Conformal geometry and brain flattening*, MICCAI, pages 271–278, 1999.

[3] E. ARBARELLO, M. CORNALBA, P. GRIFFITHS, AND J. HARRIS, *Topics in the Theory of Algebraic Curves*, 1938.

[4] T. DUCHAMP, A. CERTIAN, A. DEROSE, AND W. STUETZLE, *Hierarchical computation of pl harmonic embeddings*, preprint, 1997.

[5] X. Gu, Y. Wang, T. Chan, P.M. Thompson, and S.-T. Yau, *Brain surface conformal mapping*, In: Human Brain Mapping, 2003.

[6] X. Gu, Y. Wang, T. Chan, P. M. Thompson, and S.-T. Yau, *Genus zero surface conformal mapping and its application to brain surface mapping*, In: Information Processing in Medical Imaging, 2003.

[7] X. Gu and S.-T. Yau, *Computing conformal structures of surafces*, Communication of Informtion and Systems, 2:2(2002), pp. 121–146.

[8] X. Gu and S.-T. Yau, *Global conformal surface parameterization*, In: ACM Symposium on Geometry Processing, pages 127–137, 2003.

[9] X. Gu and S.-T. Yau, *Surface classification using conformal structures*, In: International Conference on Computer Vision, pages 701–708, 2003.

[10] S. Haker, S. Angenent, A. Tannenbaum, R. Kikinis, G. Sapiro, and M.Halle, *Conformal surface parameterization for texture mapping*, IEEE Transactions on Visualization and Computer Graphics, 6(2000), pp. 240–251.

[11] I. Kra and H. M. Farkas, *Riemann Surfaces*. Springer-Verlag New York, Incorporated, 1995.

[12] B. Levy and J. L. Mallet, *Non-distorted texture mapping for sheared triangulated meshes*, In: SIGGRAPH 98, pages 343–352.

[13] B. Levy, S. Petitjean, N. Ray, and J. Maillot, *Least squares conformal maps for automatic texture atlas generation*, In: SIGGRAPH 02, pages 362–371, 2002.

[14] Y. Wang, X. Gu, T. Chan, P. M. Thompson, and S.-T. Yau, *Intrinsic brain surface conformal mapping using a variational method*, In: SPIE International Symposium on Medical Imaging, 2004.